

Maia variables and other anomalies among pulsating stars

L. A. Balona^{*}

¹ *South African Astronomical Observatory, P.O. Box 9, Observatory 7935, South Africa*

Accepted Received ...

ABSTRACT

From *TESS* photometry, 493 mid- to late-B stars with high frequencies (Maia variables) have been identified. The distribution of projected rotational velocities shows that the rotation rates of Maia variables are no different from those of SPB stars. Moreover, many Maia stars pulsate with frequencies exceeding 60 d^{-1} . Rapid rotation is ruled out as a possible factor in understanding the Maia variables. There is clearly a serious problem with current pulsational models. Not only are the models unable to account for the Maia stars, they fail to account for the fact that SPB and γ Dor variables form one continuous instability strip from the cool end of the δ Sct region to the hot end of the β Cep instability strip. Likewise, there is continuity between the distributions of δ Sct, Maia and β Cep variables. In fact, Maia stars seem to be an extension of δ Sct stars to mid-B type. These observations suggest an interplay between multiple driving mechanisms rather than separate dominant mechanisms for each variability group.

Key words: stars: early-type – stars: oscillations – stars: variables: general

1 INTRODUCTION

The Maia variables are defined as pulsating stars with high frequencies which are too hot to be classified as δ Scuti stars and too cool to be β Cephei variables. These anomalous pulsating stars have been suspected for many decades following a report by [Struve \(1955\)](#) of short-period variations in the star Maia, a member of the Pleiades cluster. [Struve et al. \(1957\)](#) later disclaimed the variability. It is now known from the *K2* space mission that Maia itself is a rotational variable with a 10-d period ([White et al. 2017](#)) and no sign of high frequencies. Recently, however, [Monier \(2021\)](#) has reported rapid light variations in the far ultraviolet.

In the past, ground-based observations by [McNamara \(1985\)](#), [Lehmann et al. \(1995\)](#), [Percy & Wilson \(2000\)](#) and [Kallinger et al. \(2004\)](#) indicated that Maia variables might exist, even though models do not predict pulsational instability. From *CoRoT* observations, [Degroote et al. \(2009\)](#) found several low-amplitude B-type pulsators between the SPB and δ Sct instability strips, with a very broad range of frequencies and low amplitudes.

[Mowlavi et al. \(2013\)](#) provided further evidence for Maia variables. They found that many rapidly rotating mid-B stars in the open cluster NGC 3766 pulsate with frequencies as high as 10 d^{-1} . [Mowlavi et al. \(2016\)](#) also found that the majority of these stars obey a period–luminosity relation. They suggested the name “FaRPB” for these stars.

However, their properties are similar to what have been historically called the Maia variables.

Several B stars qualifying as Maia variables have been detected in the *Kepler* field ([Balona et al. 2015, 2016](#)). Using *TESS* data, [Balona & Ozuyar \(2020\)](#) identified 131 Maia candidates. More recently [Gaia Collaboration et al. \(2022\)](#) found a population of Maia stars using *Gaia* photometry. They interpret the high frequencies as an effect of rapid rotation in SPB stars.

From *TESS* observations, [Balona & Ozuyar \(2020\)](#) found that stars pulsating at frequencies higher than about 5 d^{-1} are common among all B stars, including late-B and early A stars. Furthermore, there are no distinct regions of instability as expected from the models. The β Cep variables merge smoothly with Maia stars which merge smoothly into δ Sct stars. The same occurs for the low-frequency pulsators. SPB stars are found all along the B-type main sequence and continue into the A star region where they merge with the hot γ Dor variables. As a result, rather arbitrary effective temperature and frequency limits had to be introduced in order to define the different variability groups.

Using *TESS* photometry, [Sharma et al. \(2022\)](#) confirmed the continuity of SPB pulsations to cooler temperatures extending into the A stars. They suggested that these might be rapidly rotating SPB stars. Rotation and uncertainties in effective temperature obviously contribute to the blurring of distinct instability regions, but it is still surprising that the concentration of stars in their respective domains of instability expected from the models is

* E-mail: lab@sao.ac.za

not seen, despite the large numbers of early-type pulsating stars discovered by *TESS*. This is evident from Fig 2 of Balona & Ozuyar (2020).

When observed equator-on, rapid rotation lowers the apparent effective temperature due to equatorial gravity darkening, shifting the star to cooler temperatures in the H–R diagram. A rapidly-rotating β Cep star could, for example, be mistaken for a Maia variable. Furthermore, gravito-inertial modes in moderate to fast rotators may have frequencies higher than normal. Thus a rapidly-rotating SPB star may also be mistaken for a Maia variable. Salmon et al. (2014) investigated these effects and concluded that their models could reproduce the observations of Mowlavi et al. (2013, 2016).

Saio et al. (2017) examined pulsation models of rapidly-rotating main sequence B stars and calculated the properties of prograde sectoral g and retrograde r modes excited by the κ mechanism at the Fe opacity peak. They found that the period-luminosity relation described by Mowlavi et al. (2016) can be explained by prograde sectoral g modes of rapidly rotating stars.

Daszyńska-Daszkiewicz et al. (2017) considered three hypothesis for the Maia variables: rapidly rotating stars with underestimated masses, rapidly rotating stars with non-standard opacities and slowly rotating stars with non-standard opacities. While there are indications that one or more of these hypotheses might be able to explain the observations, no definite conclusions can be made at this stage.

It is clear that the most common opinion is that Maia variables are simply rapidly rotating SPB stars. It is therefore important to test this idea by comparing the rotation rate of Maia stars with the rotation rate of SPB stars using the respective distributions of projected rotational velocities. Such a test was performed by Balona & Ozuyar (2020) using 41 Maia stars, but no significant difference in rotation rate between Maia stars and main sequence stars could be found. However, the sample of Maia stars is rather small for a definitive conclusion.

In this paper, we use *TESS* data from Sectors 1–59 to identify new Maia candidates as well as other pulsating A and B stars. Full details of how the search was conducted, how estimates of effective temperature were obtained and the sources of projected rotational velocities are described in Balona (2022a). The larger numbers of variable stars also allow a better examination of the boundaries between various variability groups which have been historically defined by their different pulsation mechanisms. It is show that the concept of distinct instability strips is not valid and that the blending of these groups cannot simply be attributed to rapid rotation or uncertainties in effective temperature.

2 NEW MAIA VARIABLES

The *TESS* mission has been observing the whole sky and obtaining light curves for thousands of stars with two-minute cadence. This wide-band photometry has been corrected for long-term drifts using pre-search data conditioning (PDC, Jenkins et al. 2010). The author has been engaged in a project to classify the variability of stars hotter than about 6000 K. Results of the classification of over 120000 stars, together with their effective temperatures, T_{eff} , luminosities,

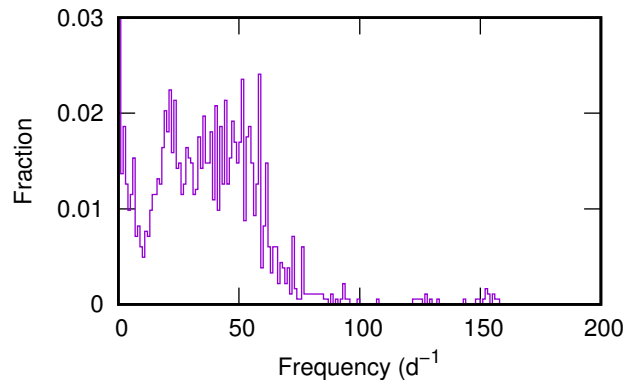


Figure 1. Frequency distribution in Maia stars.

$\log L/L_{\odot}$, and projected rotational velocities, $v \sin i$, are reported in Balona (2022a). The values of $\log L/L_{\odot}$, are from Gaia DR3 parallaxes (Gaia Collaboration et al. 2016, 2018).

During this process, many stars were detected which normally would be classified as δ Sct variables, but with effective temperatures in the range 10000–18000 K. These were classified as Maia variables if frequency peaks higher than $\nu_{\text{min}} = 5 \text{ d}^{-1}$ were detected. The choices of T_{eff} range and ν_{min} are arbitrary, but are guided by the fact that most SPB stars have frequencies not much higher than about 3 d^{-1} . The full list of 493 Maia stars (and other variables) is to be found in Balona (2022a). In the present work, only stars within the main-sequence band are considered. This band is defined by $-0.5 < \Delta \log L/L_{\odot} < 1.5$, where $\Delta \log L/L_{\odot}$ is the luminosity above the zero-age main sequence. Out of the 493 Maia variables, 420 stars are located within this main sequence band.

The choice of ν_{min} is not too important. With $\nu_{\text{min}} = 5 \text{ d}^{-1}$, 420 stars are classified as Maia variables. If $\nu_{\text{min}} = 10 \text{ d}^{-1}$ is used, then 351 stars are Maia variables, but then one needs to modify the definition of SPB stars to include this new upper frequency limit. Clearly, most Maia variables have frequencies higher than 10 d^{-1} .

On the other hand, the boundary between SPB and β Cep stars is not at all well defined. Some bright, well-known β Cep stars have frequencies lower than 4 d^{-1} , in which case these would be considered as SPB variables according to the above definition with $\nu_{\text{min}} = 5 \text{ d}^{-1}$. To allow for this, the frequency limit for SPB stars with $T_{\text{eff}} \geq 18000 \text{ K}$ was lowered to $\nu_{\text{min}} = 3 \text{ d}^{-1}$. Thus in Balona & Ozuyar (2020) and Balona (2022a), as well as in this work, the definition for SPB variables depends on whether the effective temperature is greater or lower than 18000 K. Sharma et al. (2022) encountered the same difficulty, and set $\nu_{\text{min}} = 2.4 \text{ d}^{-1}$ to distinguish between SPB and β Cep variables.

The actual frequency distribution in Maia variables is shown in Fig. 1. This figure was constructed from frequency peaks with signal-to-noise ratio $S/N > 5.0$ irrespective of amplitude. Frequencies between $20\text{--}50 \text{ d}^{-1}$ are quite common. It is clear that such high frequencies in mid-B stars are incompatible with current models. In their models of rapidly rotating SPB stars, Salmon et al. (2014) do not find any instance of pulsations with frequencies higher than 10 d^{-1} .

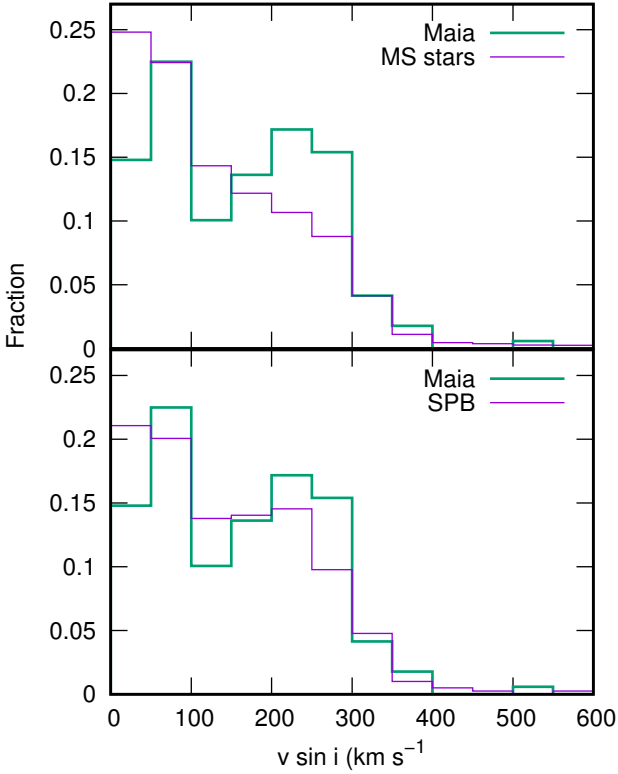


Figure 2. Top panel: the distribution of projected rotational velocity, $v \sin i$, for Maia variables (heavy green histogram) and for main sequence stars in the same temperature range. The bottom panel shows the distributions for Maia and SPB stars in the same temperature range.

This is already an indication that rapid rotation should be discounted as an explanation for the Maia variables.

There are quite a few Maia stars which pulsate at rather high frequencies. In fact, they would probably be mistaken for roAp stars, except that they are of type B and non-peculiar. The roAp stars themselves can no longer be considered a separate class (Balona 2022b). As described in Balona (2022a), the class MAIAH is given if the highest frequency peak lies in the range $50\text{--}60 \text{ d}^{-1}$, while if it is higher than 60 d^{-1} , the notation MAIAU is used. This does not indicate a separate class, but is a convenient way of identifying Maia stars with these peculiar high frequencies. A total of 90 high-frequency Maia variables are listed in Table 1. This consists of 43 MAIAH and 47 MAIAU stars.

3 ROTATION

As already mentioned, rotation affects the apparent location of the star in the H–R diagram due to equatorial gravity darkening and introduces new gravito-inertial modes with moderately high frequencies (Salmon et al. 2014). Gravity darkening will occur in all stars, whether pulsating or not. Therefore no bias is introduced in comparing the rotational velocities of Maia stars with main sequence stars in the same effective temperature range.

The distribution of projected rotational velocities, $v \sin i$, for 169 Maia stars and for 6546 main sequence stars

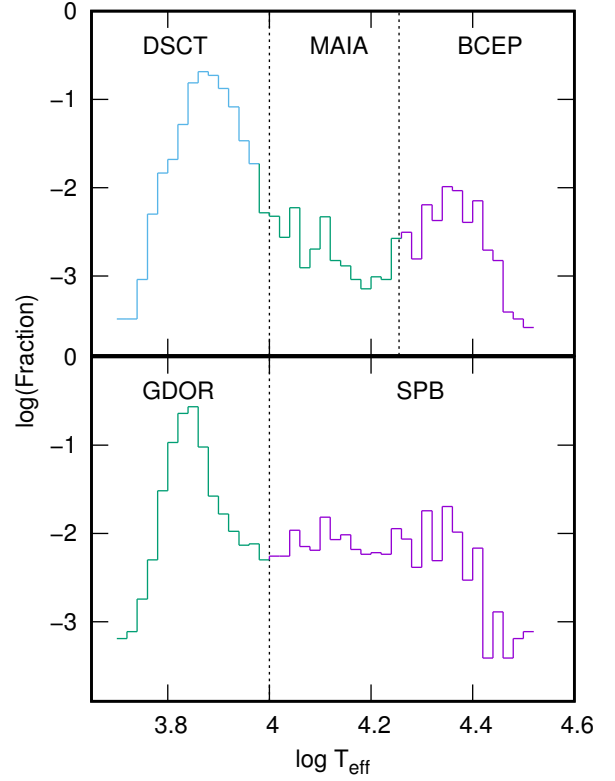


Figure 3. The distribution of δ Sct, Maia and β Cep variables (top panel) and the γ Dor and SPB stars (bottom panel).

in the temperature range ($10000 < T_{\text{eff}} < 18000$) is shown in Fig. 2. Also shown in the same figure is a comparison with 399 SPB stars in the same temperature range. The conclusion is clear: Maia stars are not rapidly rotating SPB stars. The rotation rates of both Maia and SPB stars are the same as in normal main sequence stars.

4 DISTRIBUTION OF MAIA STARS

Fig. 3 shows the number density of δ Sct, Maia and β Cep as well as γ Dor and SPB variables as a function of effective temperature. This figure was constructed by counting the number of stars of a particular variability class within a small range of effective temperature (0.02 dex in $\log T_{\text{eff}}$) within the main sequence band as previously defined.

The figure illustrates the problem pointed out by Balona & Ozuyar (2020): there are no distinct instability regions among hot stars. There is no doubt that uncertainty in the effective temperature must be partly responsible. The typical uncertainty in $\log T_{\text{eff}}$ is about 0.02 dex (which is the bin size in the figure), so it seems unlikely to be the sole reason. The figure also appears to suggest that Maia stars are not a separate class, but simply an extension of the δ Sct variables to mid-B spectral types. On this basis one could rename Maia variables as “hot δ Sct stars” or something similar. However, this would be contrary to the spirit of classification in which stars of a particular group pulsate with the same mechanism.

Fig. 3 shows that the γ Dor and SPB variables form a

Table 1. List of Maia variables with high frequencies. These are classified as MAIAH if the maximum frequency $\nu_{\max} < 60 \text{ d}^{-1}$ and as MAIAU if $\nu_{\max} > 60 \text{ d}^{-1}$. The number of frequencies greater than 50 d^{-1} , N , is also shown as well as the effective temperature, T_{eff} (in K) and the luminosity, $\log \frac{L}{L_{\odot}}$. The last column is the spectral type.

TIC	Var Type	ν_{\max}	N	T_{eff}	$\log \frac{L}{L_{\odot}}$	Sp. Type	TIC	Var Type	ν_{\max}	N	T_{eff}	$\log \frac{L}{L_{\odot}}$	Sp. Type
10433563	MAIAH	58.24	1	11300	2.14	B9.5V	262566258	MAIAH	58.76	1	11300	1.79	B9
27804376	MAIAU	60.52	2	11300	1.48	B9/A1IV/V	263261751	MAIAH	53.59	1	12600	1.75	B8:
30965889	MAIAU	60.97	1	10174	1.14	A0	264540595	SPB+MAIAH	50.22	2	11164	1.87	B9.5V
38127832	MAIAH+SXARI	54.56	6	12500	2.68	B9pSi	282742134	MAIAH	53.26	11	11300	1.25	B9
52831545	MAIAU+ROT	53.29	17	10053	1.16	A2	284163505	MAIAH+ROT	53.31	2	10257	2.03	B9.5Vp
52844490	MAIAH	51.64	7	10047	1.14	A2	284473460	MAIAU	51.32	7	11300	1.61	B9
60245596	MAIAH	54.18	2	14000	2.16	B7/8IV	284935176	MAIAH	72.21	3	11300	1.32	B9
74214081	MAIAU	93.77	1	11273	1.35	A0V	286344698	MAIAU	72.73	1	10518	1.30	A2V
76138809	MAIAU	62.31	4	11245	2.38	B9III	293290586	MAIAU+ROT	156.89	1	12600	2.89	B8/9IV/V
86703658	MAIAU	68.63	1	17500	2.96	B5V	299123331	MAIAH	52.29	1	10029	1.44	A0
92736909	MAIAU	62.11	2	10695	1.20	A2V	299486936	MAIAH	51.23	1	10740	1.12	A5
92780981	MAIAU	54.74	2	11300	1.40	B9	3000175097	MAIAH+ROT	58.35	6	13363	2.29	B8III
105262398	MAIAH	51.47	2	10466	1.29	A0	300493372	MAIAU	61.20	3	11220	1.38	A0
105889061	MAIAU	60.58	3	11300	1.32	B9	301100741	MAIAH+SXARI	50.18	4	17500	2.54	hB5HeB8pSi
105896213	MAIAU	67.44	2	11300	1.37	B9	304570125	MAIAU	63.79	11	10523	1.16	A0
115119794	MAIAU+ROT	63.84	6	10267	2.35	A0III/V	308769611	MAIAU	55.22	38	10116	1.68	A0V
121893547	MAIAH	53.65	1	11300	1.61	B9	315207705	MAIAU	63.91	1	17500	2.89	B5/7V:n:
124494015	MAIAU	61.37	21	11300	1.32	B9.5V	332856650	MAIAH	51.96	1	11960	2.40	B8/9
125080827	MAIAH	52.94	1	11300	2.18	B9.5IVnn	340356526	MAIAU	58.50	4	12500	2.20	B8IV/V
125977802	MAIAU	56.70	2	10903	1.63	A0V	345553381	MAIAU	70.58	1	11300	2.19	B9V
132923245	MAIAU+FLARE	78.01	1	11300	1.44	B9	352297130	MAIAU+ROT	62.99	6	11300	1.52	B9
133696007	MAIAH+SXARI	50.28	6	10843	1.85	A0Si	355775097	MAIAU	51.10	3	10744	1.33	A3/5IV:
133702466	MAIAH	53.94	1	10644	1.68	B8/A0	362653719	MAIAH	52.64	1	11300	1.36	B9
134860590	MAIAU+ROT	61.33	10	10928	1.23	A2V	363917122	MAIAH	52.91	1	10407	1.45	A2/3V
134861413	MAIAU	51.10	7	11230	1.29	A3	372913430	MAIAH	56.72	1	11772	2.22	B8.5V
136179360	MAIAU	62.44	16	11300	1.68	B9	377443211	MAIAU	61.19	1	12600	1.52	B8V
137822799	MAIAH	73.99	1	10265	2.20	B9.5III	379937109	MAIAU	50.78	35	11300	1.39	B9
144517863	MAIAU	52.95	17	12151	2.20	B9V	387757610	MAIAH	54.86	7	10422	1.53	A2
144710346	MAIAU	55.58	4	10460	1.16	A3	388688820	MAIAU	50.15	14	10089	1.26	A3
144956901	MAIAH	57.33	2	13700	3.02	B7III	391154611	MAIAH	51.52	4	10300	1.54	B9V
145923579	MAIAU	62.88	2	10435	1.66	B9IV-Vkn	391346342	SPB+MAIAU	59.59	3	13932	2.74	B6Vnn
174662768	SPB+MAIAH	50.64	3	14062	2.71	B5Vn	401536404	MAIAH	53.17	1	10298	2.16	B9.5Vn
174866532	MAIAH	51.87	1	10288	1.19	A2	401785909	MAIAU+ROT	52.66	5	10638	1.24	A2
182910557	MAIAU	60.43	1	10063	1.20	A3/5	403787892	MAIAH+EA	57.32	7	16143	3.30	B5III
183522571	MAIAU	60.16	5	10799	1.45	A1/2IV/V	415545142	MAIAH	55.56	2	10184	1.29	A2
196500681	MAIAH	52.07	1	11100	1.62	B9.5V	416635930	MAIAH+EB	51.03	6	12331	2.55	B9IV-V
202121249	MAIAH	51.49	4	11300	1.30	B9-V	419367293	MAIAH	51.98	1	11300	2.24	B9V
202431888	MAIAU	74.11	1	12023	2.53	B9IVS:	421714420	MAIAU+EA	53.15	6	12600	2.33	B8
220313579	MAIAU	61.50	9	10014	1.35	A2/3	422454176	MAIAH+ROT	50.46	2	12600	1.51	B8.5V
233110625	MAIAH	52.56	1	10199	1.57	A2	429306233	MAIAU	54.76	5	10000	1.79	A0p(Si)
233310793	MAIAH	51.90	21	12678	1.55	A5-F5	440638544	MAIAU	58.58	6	10561	1.18	A0
236785664	MAIAU+BE+ROT	56.97	4	11300	2.45	B9Ve	447086833	MAIAH	50.38	1	11300	1.45	B9/A1V
238317411	MAIAU+ROT	69.52	1	11300	2.20	B9IV	450784713	MAIAU+ROT	58.43	14	10128	1.79	B9/A0
238641255	MAIAU+ROT+FLARE	61.82	25	10137	1.21	A1V	464470984	MAIAH+ROT	59.70	1	11066	2.17	B9IV/V
251058870	MAIAH	54.75	4	11300	2.26	B9III:nn	469421586	MAIAH+BE+ROT	53.86	1	12600	2.91	B8IV/V

continuous group, quite unlike predictions from stellar models. Moreover, it has been established that the γ Dor instability region lies within the δ Sct instability region (Balona 2018), further eroding the idea that different stellar variability classes are associated with different pulsation mechanisms.

As already mentioned, Sharma et al. (2022) suggested that gravity darkening due to rapid rotation might explain B-type low-frequency pulsators too cool to be SPB stars. To test this idea, we examined the $v \sin i$ distribution of 60 low-frequency pulsators with $9000 < T_{\text{eff}} < 11000$ K and compared it to the $v \sin i$ distribution of 1217 main sequence stars in the same effective temperature range. There is no obvious difference between the distributions, but the sample is rather small. For SPB stars, the mean is $\langle v \sin i \rangle = 159 \pm 12 \text{ km s}^{-1}$ and for main sequence stars $\langle v \sin i \rangle = 118 \pm 2 \text{ km s}^{-1}$. In any case the rotation rate of these hot γ Dor/SPB variables cannot be called rapid.

Pulsations in δ Sct stars are driven by the opacity κ mechanism operating in the He II ionization zone. This mechanism does not work for effective temperatures as high as $T_{\text{eff}} \approx 16000$ K, which, judging from Fig. 3, is the highest temperature for pulsation in Maia stars. According to the latest models, pulsational driving of low degree modes

in δ Sct stars does not occur for $T_{\text{eff}} > 9000$ K (Xiong et al. 2016). According to current models, Maia stars cannot be considered as high temperature δ Sct stars, nor can they be explained as rapidly rotating SPB stars.

5 CONCLUSIONS

From *TESS* light curves, 493 stars have been identified as Maia variables. These are defined as main sequence stars with $10000 < T_{\text{eff}} < 18000$ K and frequencies greater than 5 d^{-1} . By comparing the projected rotational velocities of the stars with those of main sequence stars or SPB variables in the same temperature range, it is shown that Maia stars are not rapidly rotating. Therefore the idea that the high frequencies in Maia variables are due to rapid rotation (Salmon et al. 2014) is refuted. Moreover, such an idea cannot explain frequencies of over 50 d^{-1} seen in many Maia stars.

It is also demonstrated that there is no clear separation in effective temperature between δ Sct and Maia variables or between β Cep and Maia variables. Indeed, as Fig. 3 shows, there is no clear separation between any variability group among early-type stars, as already pointed out in

Balona & Ozuyar (2020). The sequence of SPB stars, which begins at about spectral type B0, runs all the way to A0 where it merges with the sequence of γ Dor stars running towards the cool end of the δ Sct instability strip (the hot γ Dor variables, Balona et al. 2016). The largest concentration of γ Dor stars occurs around $T_{\text{eff}} \approx 7000$ K. The instability strip defined by the majority of γ Dor stars actually lies within the δ Sct instability strip, as pointed out by Balona (2018), which is very puzzling.

Sharma et al. (2022) suggested that low frequency stars between the SPB and δ Sct instability strips are probably SPB stars shifted to cooler temperatures owing to gravitational darkening at the equator as a result of rapid rotation. This is not supported by a comparison of their projected rotational velocities with those of main sequence stars in the same effective temperature range. These low frequency late-B stars merge into the hot γ Dor variables. Rapid rotation certainly cannot be an explanation for the hot γ Dor stars, since the required apparent temperature shift due to equatorial gravity darkening is far too large.

While uncertainties in T_{eff} , different metallicities and other factors may be partly responsible for the lack of well-defined instability regions, it seems unlikely that these are the sole causes. There is clearly something wrong with current pulsation models. Since the models cannot explain the easily identifiable γ Dor, δ Sct, SPB, Maia and β Cep stars, it is difficult to place much trust on models involving deep internal core pulsations (e.g. Lee & Saio 2020).

It is possible that there may be an interplay of different driving mechanisms which vary in effectiveness. The discovery that starspots are pervasive along the entire main sequence (Balona 2022c) is relevant. This seems to imply that surface convection present in all A and B stars. Including convection in the models may assist in resolving these problems, but convection may not be the only factor.

A better understanding of the upper stellar layers of A and B stars is required in order to improve the pulsation models. Therefore, an in-depth study of the causes of rotational light modulation is required. In order to understand the roAp-like frequencies in some Maia stars (Table 1), modes of high degree should receive particular attention.

ACKNOWLEDGMENTS

LAB wishes to thank the National Research Foundation of South Africa for financial support and Dr Tim Bedding for useful comments.

Funding for the *TESS* mission is provided by the NASA Explorer Program. Funding for the *TESS* Asteroseismic Science Operations Centre is provided by the Danish National Research Foundation (Grant agreement no.: D NRF106), ESA PRODEX (PEA 4000119301) and Stellar Astrophysics Centre (SAC) at Aarhus University.

This work has made use of data from the European Space Agency (ESA) mission Gaia, processed by the Gaia Data Processing and Analysis Consortium (DPAC). Funding for the DPAC has been provided by national institutions, in particular the institutions participating in the Gaia Multilateral Agreement.

This research has made use of the SIMBAD database, operated at CDS, Strasbourg, France. Data were obtained

from the Mikulski Archive for Space Telescopes (MAST). STScI is operated by the Association of Universities for Research in Astronomy, Inc., under NASA contract NAS5-2655.

DATA AVAILABILITY

All data are incorporated into the article is available though the author and described in Balona (2022a).

REFERENCES

- Balona L. A., 2018, *MNRAS*, **479**, 183
 Balona L. A., 2022a, arXiv e-prints, p. arXiv:2212.10776
 Balona L. A., 2022b, *MNRAS*, **510**, 5743
 Balona L. A., 2022c, *MNRAS*, **516**, 3641
 Balona L. A., Ozuyar D., 2020, *MNRAS*, **493**, 5871
 Balona L. A., Baran A. S., Daszyńska-Daszkiewicz J., De Cat P., 2015, *MNRAS*, **451**, 1445
 Balona L. A., et al., 2016, *MNRAS*, **460**, 1318
 Daszyńska-Daszkiewicz J., Walczak P., Pamyatnykh A., 2017, in European Physical Journal Web of Conferences. p. 03013 (arXiv:1701.00937)
 Degroote P., et al., 2009, *A&A*, **506**, 471
 Gaia Collaboration et al., 2016, *A&A*, **595**, A1
 Gaia Collaboration et al., 2018, *A&A*, **616**, A1
 Gaia Collaboration et al., 2022, arXiv e-prints, p. arXiv:2206.06075
 Jenkins J. M., et al., 2010, *ApJ*, **713**, L87
 Kallinger T., Iliev I., Lehmann H., Weiss W. W., 2004, in J. Zverko, J. Ziznovsky, S. J. Adelman, & W. W. Weiss ed., IAU Symposium Vol. 224, The A-Star Puzzle. pp 848–852
 Lee U., Saio H., 2020, *MNRAS*, **497**, 4117
 Lehmann H., Scholz G., Hildebrandt G., Kloze S., Panov K. P., Reimann H.-G., Woche M., Ziener R., 1995, *A&A*, **300**, 783
 McNamara B. J., 1985, *ApJ*, **289**, 213
 Monier R., 2021, *Research Notes of the American Astronomical Society*, **5**, 81
 Mowlavi N., Barblan F., Saesen S., Eyer L., 2013, *A&A*, **554**, A108
 Mowlavi N., Saesen S., Semaan T., Eggenberger P., Barblan F., Eyer L., Ekström S., Georgy C., 2016, *A&A*, **595**, L1
 Percy J. R., Wilson J. B., 2000, *PASP*, **112**, 846
 Saio H., Ekström S., Mowlavi N., Georgy C., Saesen S., Eggenberger P., Semaan T., Salmon S. J. A. J., 2017, *MNRAS*, **467**, 3864
 Salmon S. J. A. J., Montalbán J., Reese D. R., Dupret M.-A., Eggenberger P., 2014, *A&A*, **569**, A18
 Sharma A. N., Bedding T. R., Saio H., White T. R., 2022, *MNRAS*, **515**, 828
 Struve O., 1955, *Sky & Telesc.*, **14**, 461
 Struve O., Sahade J., Lynds C. R., Huang S. S., 1957, *ApJ*, **125**, 115
 White T. R., et al., 2017, *MNRAS*, **471**, 2882
 Xiong D. R., Deng L., Zhang C., Wang K., 2016, *MNRAS*, **457**, 3163